Arnold Mathematical Journal (2021) 7:341–355
https://doi.org/10.1007/s40598-021-00174-y

PROBLEM CONTRIBUTION

Fifty New Invariants of N-Periodics in the Elliptic Billiard

Dan Reznik[1] · **Ronaldo Garcia**[2] · **Jair Koiller**[3]

Received: 8 May 2020 / Revised: 21 October 2020 / Accepted: 4 January 2021 /
Published online: 18 February 2021
© Institute for Mathematical Sciences (IMS), Stony Brook University, NY 2021

Abstract
We introduce 50+ new invariants manifested by the dynamic geometry of N-periodics in the Elliptic Billiard, detected with an experimental/interactive toolbox. These involve sums, products and ratios of distances, areas, angles, etc. Though curious in their manifestation, said invariants do all depend upon the two fundamental conserved quantities in the Elliptic Billiard: perimeter and Joachimsthal's constant. Several proofs have already been contributed (references are provided); these have mainly relied on algebraic geometry. We very much welcome new proofs and contributions.

Keywords Elliptic billiard · Invariant · Optimization · Experimental

Mathematics Subject Classification 51N20 · 51M04 · 65-05

1 Introduction

The Elliptic Billiard (EB) is a special case of Poncelet's Porism [9], where the conic pair are two confocal ellipses; it, therefore, admits a 1d family of N-periodic trajectories [9,11,26] which at every vertex are bisected by the normals to the outer ellipse in the pair (hence the term "billiard"); see Fig. 1.

✉ Dan Reznik
dreznik@gmail.com

Ronaldo Garcia
ragarcia@ufg.br

Jair Koiller
jairkoiller@gmail.com

1 Data Science Consulting, Rio de Janeiro, Brazil

2 Math and Statistics Institute, Federal University of Goiás, Goiânia, Brazil

3 Federal University of Juiz de Fora, Juiz de Fora, Brazil

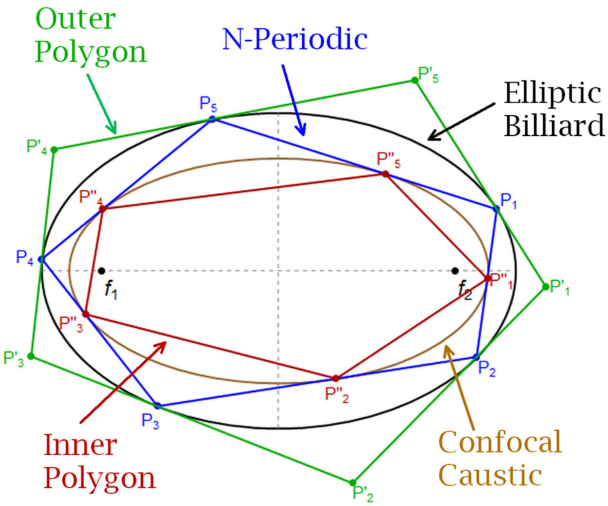

Fig. 1 A (i) 5-periodic (vertices P_i) is shown inscribed in a confocal ellipse pair (billiard and caustic). Also shown is (ii) the outer polygon with vertices P_i' tangent to the outer ellipse at the N-periodic vertices, and (iii) the inner polygon whose vertices P_i'' are at the points of contact of the N-periodic with the caustic

The EB is an *integrable* system (in fact it is conjectured as the only integrable planar billiard [12]). Integrability implies invariant perimeter L; a second classic invariant is Joachimsthal's constant J, which is simply a statement that all trajectory segments are tangent to the confocal caustic [20,26].

Continuing our work on properties of N-periodics in the EB [10,18], here we introduce 50+ newfound invariants detected via experimental exploration. These involve distances, areas, angles and centers of mass of N-periodics and associated polygons (inner, outer, pedal, antipedal, defined below). Some invariants depend on the parity of N, while others on other positional constraints.

Note that since the N-periodics in the EB are fully defined by L, J, any "new" invariants listed here or elsewhere must be ultimately dependent upon said quantities. Nevertheless, proving a specific functional dependence may require creativity. Several proofs have already been contributed and are referenced below. We hope to motivate more contributions and/or new discoveries.

This article is organized as follows: preliminary definitions are given in Sect. 2. Invariants are introduced in Sect. 3, in several clusters, involving: (i) lengths, areas, and angles of N-periodics and associated polygons; (ii) pedal polygons to N-periodics and (iii) their outer polygons; (iv) antipedal polygons (defined below); (v) area-ratios related to the Steiner curvature centroid [25]; (vi) pairs of pedal polygons; (vii) area-ratios of evolute polygons [6]; (viii) focus-inversive objects.

Details about our experimental toolbox are covered in Sect. 4. Section 5 lists videos illustrating some of the phenomena. For quick reference, all symbols used appear on Table 11 in Appendix 1. The reader is invited to visit our up-to-date and expanded list of invariants https://arxiv.org/abs/2004.12497 here.

2 Preliminaries

Let the EB have center O, semi-axes $a > b > 0$, and foci f_1, f_2 at $[\pm\sqrt{a^2-b^2}, 0]$. Let a'', b'' denote the major, minor semi-axes of the confocal caustic, whose values are given by a method due to Cayley [9], though we obtain them numerically, see Sect. 4.

As mentioned above, the perimeter L is invariant for a given N-periodic family, as is Joachmisthal's constant $J = \langle \mathcal{A}x, v\rangle$, where x is a bounce point (called P_i above), v is the unit velocity vector $(P_i - P_{i-1})/||.||$, $\langle . \rangle$ stands for dot product, and [26]:

$$\mathcal{A} = \text{diag}\left[1/a^2, 1/b^2\right]$$

Hellmuth Stachel contributed [23] an elegant expression for Joahmisthal's constant J in terms of the axes of the EB and its caustic:

$$J = \frac{\sqrt{a^2 - a''^2}}{ab}$$

Note: holding a constant, for each N, a'' and therefore J assume a distinct value.

Let a polygon have vertices $W_i, i = 1, ..., N$. In this paper, all polygon areas are *signed*, i.e., obtained from a sum of cross-products [15]:

$$\text{S} = \frac{1}{2}\sum_{i=1}^{N} W_i \times W_{i+1} \tag{1}$$

Let $W_i = (x_i, y_i)$, then $W_i \times W_{i+1} = (x_i\, y_{i+1} - x_{i+1}\, y_i)$.

The curvature κ of the ellipse at point (x, y) at distance d_1, d_2 to the foci is given by [27, Ellipse]:

$$\kappa = \frac{1}{a^2b^2}\left(\frac{x^2}{a^4} + \frac{y^2}{b^4}\right)^{-3/2} = ab(d_1d_2)^{-3/2} = (\kappa_a d_1 d_2)^{-3/2} \tag{2}$$

Where $\kappa_a = (ab)^{-2/3}$ is the constant affine curvature of the ellipse [14].

3 Invariants

In this section, we present the 56 invariants found so far in several tables. Each invariant is given an identifier k_n where the first digit of n refers to a cluster of invariants; see Table 1.

Table 1 Numbering scheme for the 56 invariants currently listed in this article

Range	Invariant group	Total
k_{101}–k_{120}	Distances, area, angles, curvature	20
k_{201}–k_{205}	N-Periodic Pedal polygons	5
k_{301}–k_{307}	Outer pedal polygon	7
k_{401}–k_{407}	Antipedal polygon	7
k_{501}–k_{503}	Steiner curvature centroid	3
k_{601}–k_{607}	Pairs of pedal polygons wrt. foci	7
k_{701}–k_{703}	Evolute polygons	3
k_{801}–k_{804}	Inversive objects	4

On the invariant tables below, column "invariant" provides an expression for the conserved quantity; column "value" provides a closed-form expression for the invariant (when available) in terms of the fundamental constants, or a '?' when not available (note that the invariant may already have been proved but no closed-form expression has yet been found); column "which N" specifies whether the invariant only holds for certain N (even, odd, etc.); column "date" specifies the month and year (mm/yy) when the invariant was first experimentally detected. Column "proven" references available proofs if already communicated and/or published, else it displays a '?'.

3.1 Basic Invariants

Invariants involving angles and areas of N-periodics and its tangential and internal polygons are shown on Table 2. There θ_i,A (resp. θ_i',A') are angles, area of an N-periodic (resp. outer polygon to the N-periodic). A'' is the area of the internal polygon (where orbit touches caustic), see Fig. 1. All sums/products go from $i = 1$ to N. $k_{101}, k_{102}, k_{103}$ originally studied in [18]. l_i and r_i denote $|P_i'' - P_i|$ and $|P_{i+1} - P_i''|$, respectively, and $d_{j,i} = |P_i - f_j|$. κ_i denotes the curvature of the EB at P_i (2). $\alpha_{j,i}$ denotes the angle $P_i f_j P_{i+1}$.

3.2 Pedal Polygons

Tables 3 and 4 describe invariants found for the *pedal polygons* of N-periodics and the outer polygon, see Fig. 2.

3.3 Pedals with Respect to N-Periodic

Let Q_i be the feet of perpendiculars dropped from a point M onto the sides of the N-periodic. Let A_m denote the area of the polygon formed by the Q_i, Fig. 2. Let ϕ_i denote the angle between two consecutive perpendiculars $Q_i - M$ and $Q_{i+1} - M$. Table 3 lists invariants so far observed for these quantities.

Table 2 Distance, area, and angle invariants displayed by the N-periodic, its outer and/or inner polygon

Code	Invariant	Value	Which N	Date	Proven
k_{101}	$\sum \cos\theta_i$	$JL - N$	All	4/19	[5,7]
k_{102}	$\prod \cos\theta_i'$	?	All	5/19	[5,7]
k_{103}	A'/A	?	odd	8/19	[5,8]
k_{104}	$\sum \cos(2\theta_i')$	?	All	1/20	[2]
k_{105}	$\prod \sin(\theta_i/2)$	?	Odd	1/20	[2]
k_{106}	$A'A$	?	Even	1/20	[8]
k_{107}	$k_{103}k_{105}$	?	$\equiv 0 \pmod 4$	1/20	?
k_{108}	k_{103}/k_{105}	?	$\equiv 2 \pmod 4$	1/20	?
k_{109}	A/A''	k_{103}	Odd	1/20	?
k_{110}	$A\,A''$	?	Even	1/20	?
k_{111}	$A'\,A''/A^2$	1	Odd	1/20	[3]
k_{112}	$A'\,A''$	$[ab/(a''b'')]^2$	All	1/20	[24]
k_{113}	$\sum d_{1,i}$	?	Even	1/20	symmetry
k_{114}	$\prod d_{1,i}$	?	$\equiv 2 \pmod 4$	4/20	?
k_{115}	$\prod \lvert P_i' - f_1\rvert$	?	$\equiv 0 \pmod 4$	4/20	?
$^\star k_{116}$	$\prod l_i / \prod r_i$	1	All	5/20	[24]
$^\star k_{117}$	$\prod l_i,\ \prod r_i$	?	Even	5/20	?
$^\star k_{118}$	$\sum l_i,\ \sum r_i$	$L/2$	Odd	8/20	?
$^\dagger k_{119}$	$\sum \kappa_i^{2/3}$	$L/[2J(ab)^{4/3}]$	All	10/20	[22]
$^\ddagger k_{120}$	$\sum \cos\alpha_{1,i}$	?	All	10/20	?

$^\star k_i, i = 116, 117, 118$ were discovered by Hellmuth Stachel
$^\dagger k_{119}$ was co-discovered with Pedro Roitman [19] and is equivalent to $k_{802,b}$
$^\ddagger k_{120}$ was suggested by A. Akopyan

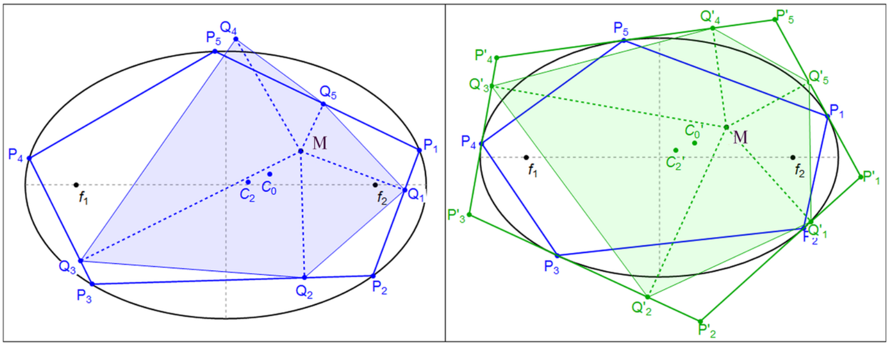

Fig. 2 Left (resp. right): Pedal polygons for $N = 5$ from a point m with respect to the N-periodic (resp. its outer polygon). Vertex and area centroids C_0, C_2 are also shown. See Videos [16, PL#01,02,03]

Table 3 Invariants of pedal polygon with respect to N-Periodic sides

Code	Invariant	Value	Which N	M	Date	Proven
$^{\dagger}k_{201}$	$\|Q_i - O\|$	a''	All	f_1, f_2	4/20	[4]
$k_{202,a}$	$\prod \|Q_i - M\|$	$(b'')^N$	Even	f_1, f_2	4/20	[7]
$k_{202,b}$	$\prod \|Q_i - M\|$	$(a''b'')^{N/2}$	$\equiv 0 \pmod 4$	O	4/20	[7]
$k_{203,a}$	$A\, A_m$	?	$\equiv 0 \pmod 4$	all	4/20	?
$k_{203,b}$	$A\, A_m$	?	$\not\equiv 2 \pmod 4$	O	4/20	?
k_{204}	A/A_m	?	$\equiv 2 \pmod 4$	All	4/20	?
k_{205}	$\sum \cos\phi_i$	?	All	All	4/20	[1]

$^{\dagger}k_{201}$ means the locus of the vertices of a pedal with respect to a focus is a circle

Table 4 Invariants of pedal polygon with respect to the sides of the outer polygon

Code	Invariant	Value	Which N	M	Date	Proven
$^{\dagger}k_{301}$	$\|Q'_i - O\|$	a	All	f_1, f_2	4/20	[4]
k_{302}	$\sum \|Q'_i - M\|^2$	?	All	All	4/20	[7]
$k_{303,a}$	$A'\, A'_m$	?	$\equiv 2 \pmod 4$	All	4/20	?
$k_{303,b}$	$A'\, A'_m$	?	$\not\equiv 0 \pmod 4$	O	4/20	?
k_{304}	A'/A'_m	?	$\equiv 0 \pmod 4$	All	4/20	?
k_{305}	$\prod \cos\phi'_i$	?	All	All	4/20	[1]
k_{306}	C'_0	?	All	All	4/20	[7]
k_{307}	C'_2	?	Even	All	4/20	?

$^{\dagger}k_{301}$ means the locus of the outer pedal with respect to a focus is a circle

3.4 Pedals with Respect to the Outer Polygon

Let Q'_i be the feet of perpendiculars dropped from a point M onto the outer polygon. Let ϕ'_i denote the angle between two consecutive perpendiculars $Q'_i - M$ and $Q'_{i+1} - M$. Let A'_m denote the area of the polygon formed by the Q'_i.

In the spirit of [21], we also analyze centers of mass: $C'_0 = \sum_i Q'_i/N$ is the vertex centroid, and the *area* centroid C'_2 of the polygon defined by the Q'_i. The area centroid $\overline{W}$ of a polygon W is given by [15]:

$$\overline{W} = \frac{1}{6S}\sum_{i=1}^{N}(W_i \times W_{i+1})(W_i + W_{i+1})$$

where W_i, S, are a polygon's vertices and its signed area, (1). Table 4 lists invariants so far observed for these quantities.

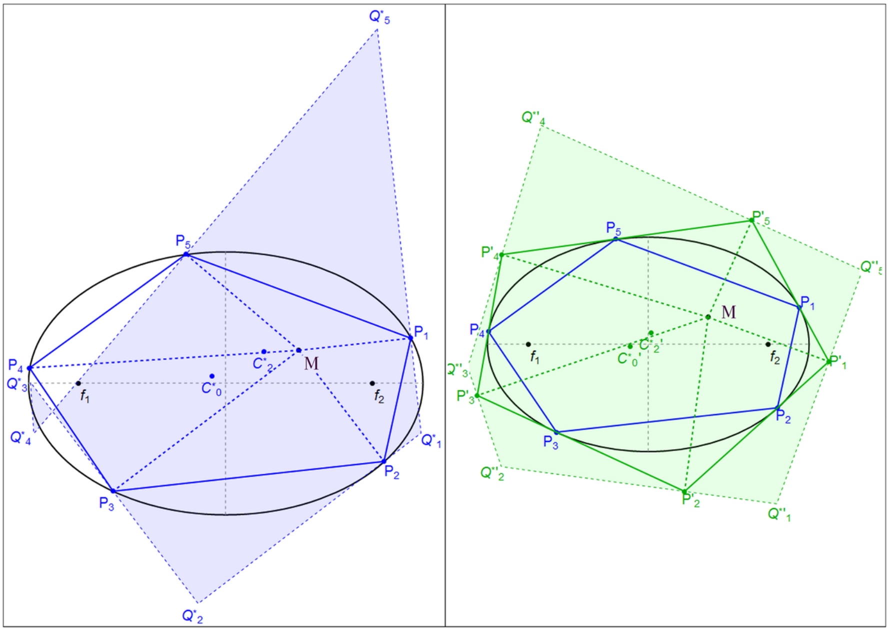

Fig. 3 Left (resp. right): antipedal polygons for $N = 5$ from a point m with respect to the N-periodic (resp. its outer polygon). Vertex and area centroids C_0^*, C_2^* are also shown

3.5 Antipedal Polygons

The antipedal polygons to the N-periodic and the outer polygon are shown in Fig. 3. The antipedal polygon Q_i^* of P_i with respect to M is defined by the intersections of rays shot from every P_i along $(P_i - M)^{\perp}$.

Let A_m denote the area of the Q_i^* polygon and C_0^*, C_2^* its vertex- and signed[1] area-centroids. $C_0'^*, C_2'^*$ refer to centers of antipedals of the outer polygon. Table 5 lists invariants found so far for these polygons.

3.6 Pedals of Steiner Curvature Centroids

Given a polygon with vertices R_i and angles θ_i, its Steiner Centroid of Curvature[2] is invariant if K is given by [25, p. 22]:

$$K = \frac{\sum_{i=1}^{N} w_i R_i}{\sum w_i}, \quad \text{with } w_i = \sin(2\theta_i)$$

[1] Antipedals can be self-intersecting.

[2] J. Steiner (following a similar result by J. Sturm in 1823 for triangles) proved in 1825 that the area of pedal polygons of a polygon R with respect to points on any given circumference centered on K [25] is invariant.

Table 5 Invariants of antipedal polygons

Code	Invariant	Value	Which N	M	Date	Proven
k_{401}	$A'\,A_m^*$	?	$\equiv 2 \pmod 4$	All	4/20	?
k_{402}	A'/A_m^*	?	$\equiv 0 \pmod 4$	All	4/20	?
$k_{403,a}$	$A_m\,A_m^*$	?	Odd	O	4/20	?
$k_{403,b}$	$A_m\,A_m^*$	?	$\equiv 0 \pmod 4$	f_1, f_2	4/20	?
k_{404}	A_m^*/A_m	?	$\equiv 2 \pmod 4$	f_1, f_2	4/20	?
k_{405}	C_0^*	?	Even	O, f_1, f_2	4/20	?
$k_{406,a}$	$C_0^{*\prime}, C_2^{*\prime}$	O	Even	O	4/20	?
$k_{406,b}$	$C_0^{*\prime}, C_2^{*\prime}$	?	4	f_1, f_2	4/20	?
k_{407}	$C_0^{*\prime}$	?	Even	f_1, f_2	4/20	?

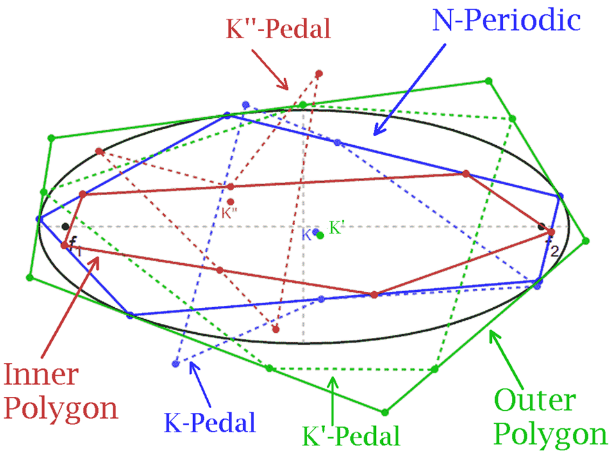

Fig. 4 An N-periodic P is shown along with its outer P' and inner P'' polygons. Also shown are their Steiner centroids of curvature K, K', K'' and the the pedal polygons P_k, P_k', P_k'' with respect to said centroids

Referring to Fig. 4, let P, P', P'' denote as before the N-periodic, outer, and inner polygons, A, A', A'' their areas, and K, K', K'' their Steiner centroids of curvature. Let P_k, P_k', P_k'' denote the pedal polygons of P, P', P'' with respect to K, K', K'', and A_k, A_k', A_k'' their areas.

When N even, the curvature centroids are stationary at the origin, so invariants described before involving A, A_m (and primed quantities) for $M = O$ apply. For odd N, the Curvature Centroids move along individual ellipses concentric with the EB. Invariants are observed appear on Table 6.

Combining the above with k_{103} and k_{106} one obtains as corollaries the fact that A_k/A_k', A_k/A_k'', and A_k'/A_k'' are invariant for odd N.

Table 6 Invariants of pedal polygons of N-periodic, outer, and inner polygons, with respect to their Steiner Curvature Centroids

Code	Invariant	Value	Which N	Date	Proven
k_{501}	A/A_k	?	Odd	7/20	?
k_{502}	A'/A'_k	?	Odd	7/20	?
k_{503}	A''/A''_k	?	Odd	7/20	?

Table 7 Invariants between pairs of pedal polygons defined with respect to the foci

Code	Invariant	Value	Which N	Date	Proven
k_{601}	$\sum q_{1,i} \sum q_{2,i}$	?	Odd	4/20	?
k_{602}	$\prod q_{1,i} \prod q_{2,i}$	?	All	4/20	?
k_{603}	$\sum q^*_{1,i} / \sum q^*_{2,i}$	1	All	5/20	?
$k_{604,a}$	A_1/A_2	1	Even	4/20	Symmetry
$k_{604,b}$	A'_1/A'_2	1	Even	4/20	Symmetry
k_{605}	$A_1\, A_2$	?	Odd	4/20	?
k_{606}	$A'_1\, A'_2$	?	Odd	4/20	?
k_{607}	$A_1/A_2 = A'_1/A'_2$	?	All	4/20	?

3.7 Pairs of Focal Pedal and Antipedal Polygons

Let $Q_{1,i}$ and $Q_{2,i}$ be the vertices of the pedal polygon with respect to f_1 and f_2. Define $q_{1,i} = |Q_{1,i} - f_1|$ and $q_{2,i} = |Q_{2,i} - f_2|$. Likewise, let $Q^*_{1,i}$ and $Q^*_{2,i}$ be the vertices of the antipedal polygon with respect to f_1 and f_2. Define $q^*_{1,i} = |Q^*_{1,i} - f_1|$ and $q^*_{2,i} = |Q^*_{2,i} - f_2|$.

Let A_1 (resp. A_2) denote the area of the polygon formed by the feet of perpendiculars dropped from f_1 (resp. f_2) onto the N-periodic, and A'_1, A'_2 the same but with respect to the outer polygon. Table 7 list invariants so far detected involving pairs of these quantities.

Note $k_{604,a}$, $k_{604,b}$ can be proven via a symmetry argument, namely, area pair are equal since opposite vertices of an even N-periodic are reflections about the origin, as will be the pedal polygons from either focus.

Though not yet checked, we expect area ratio and product invariants similar to those listed on Table 7 to hold for pairs of antipedal polygons with respect to the foci, e.g., A^*_1, A^*_2 and A'^*_1, A'^*_2

3.8 Evolute Polygons

After [6], let the evolute[3] polygon R_{ev} of a generic polygon R have vertices at the intersections of successive pairs of perpendicular bisectors to the sides of R; see Fig. 5. So P_{ev}, P'_{ev}, P''_{ev} denote the evolute polygons of P, P', and P'', respectively, and A_{ev}, A'_{ev}, A''_{ev} their areas. Trivially, at $N = 3$, the latter vanish since perpendicular

[3] The evolute of a smooth curve is the envelope of the normals [27, Evolute]. The perpendicular bisector is its discrete version.

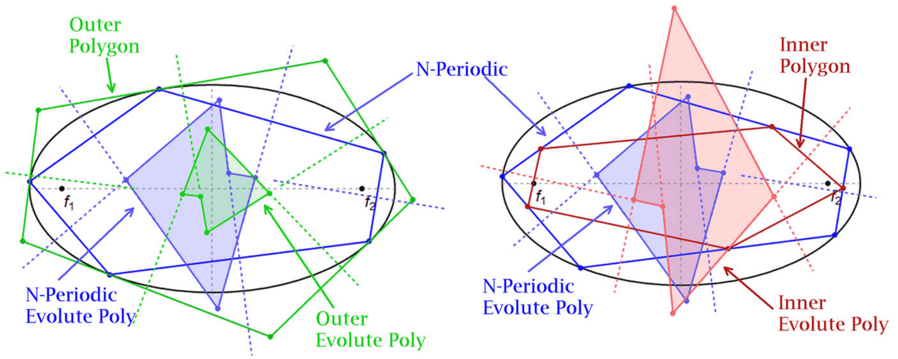

Fig. 5 **Left:** An N-Periodic and its outer polygon are shown along their evolute polygons whose vertices are ordered intersections of perpendicular bisectors. **Right:** N-periodic, inner polygon, and their evolute polygons

Table 8 Area-ratio invariants displayed by the evolute polygons of N-periodic, outer, and inner polygons

Code	Invariant	Value	Which N	Date	Proven
k_{701}	A/A_{ev}	?	> 4	7/20	?
k_{702}	A'/A'_{ev}	?	> 4	7/20	?
k_{703}	A''/A''_{ev}	?	> 4	7/20	?

Table 9 Invariants of inversive objects over the N-periodic family. As observed by A. Akopyan

Code	Invariant	Value	Which N	Date	Proven
k_{801}	$\sum d_{1,i}^{-1}/\sum d_{2,i}^{-1}$	1	All	10/20	From $k_{802,a}$
$k_{802,a}$	$\sum d_{1,i}^{-1}$	?	All	10/20	[5,19]
$^{\dagger}k_{802,b}$	$\sum 1/(d_{1,i}\, d_{2,i})$	$L/[2J(ab)^{1/2}]$	All	10/20	[22]
k_{803}	L_j	?	All	10/20	?
$^{\star}k_{804}$	$\sum \cos\gamma_{1,i}$	?	All	10/20	?

$^{\dagger}k_{802,b}$ is in fact equivalent to k_{119}, see (2)
$^{\star}k_{804}$ was co-discovered with Pedro Roitman [19]

bisectors concur. At $N = 4$, P' is a rectangle, so $A'_{ev} = 0$. Area invariants observed for $N > 4$ appear on Table 8.

Combining the above with k_{103} and k_{106} one obtains as corollaries the fact that A_{ev}/A'_{ev}, A_{ev}/A''_{ev}, and A'_{ev}/A''_{ev} are invariant for all $N > 4$.

3.9 Inversive Objects

Referring to Fig. 6, let $P_{j,i}^{-1}$ denote the inversion of P_i with respect to a unit-radius circle centered on focus f_j, $j = 1, 2$, and $d_{j,i} = |P_i - f_j|$. Let $\mathcal{P}_j$ denote the polygon whose vertices are the $P_{j,i}^{-1}$. Let L_j denote the perimeter of $\mathcal{P}_j$, and $\gamma_{j,i}$ the angles internal to $\mathcal{P}_j$'s ith vertex. Table 9 lists invariants for these and other inversive objects.

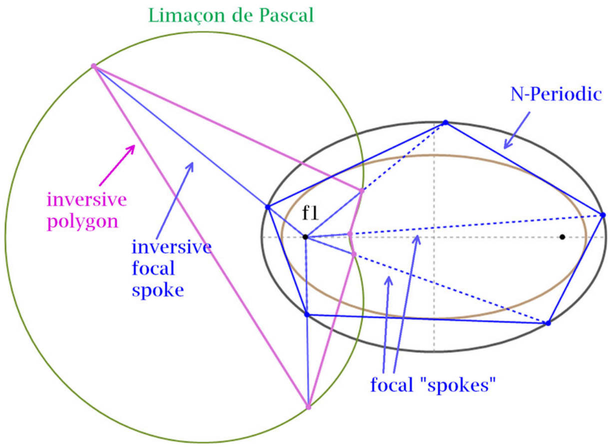

Fig. 6 The vertices of the inversive polygon are obtained by inverting N-periodic vertices with respect to a focus. Segments connecting said focus to the original (inverted) vertices are called focal spokes (resp. inversive focal spokes)

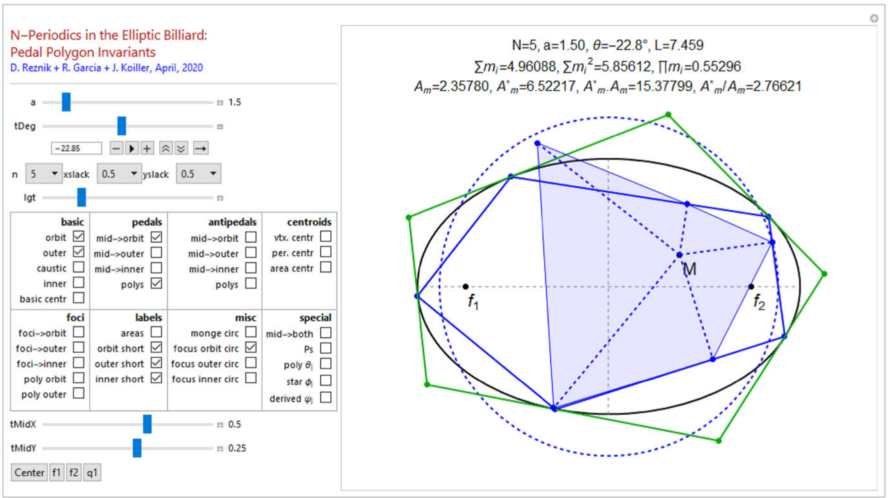

Fig. 7 Interactive toolbox written in Wolfram Mathematica [28]. The area on the left permits selection of specific geometries, whereas on the right, the EB, the N-Periodic and derived polygons is displayed. See Videos on Table 10

4 Experimental Method

An interactive toolbox was developed in Wolfram Mathematica [28] to accurately calculate and display N-periodics while reporting their areas, angles, etc., and those of some derived objects (pedal and inversive polygons, etc.); see Fig. 7.

Since all trajectories in the Billiard family are tangent to the same caustic, a crucial calculation is to obtain the caustic semiaxes a'', b'' for a given choice of a, b, and N.

Table 10 Youtube list of videos about invariants of N-Periodics, the last column provides the link

Id	Title	N	youtu.be/...
01	Area Invariants of Pedal and Antipedal Polygons	3	LN623VjeeFQ
02	Exploring invariants of N-Periodics and pedal polygons	3–12	2yXbOV7qf7k
03	Centroid Stationarity of Pedal Polygons	even	j_GD_g8aIbg
04	Equal sum of distances from foci to vertices of Antipedal Polygon	3–6	6F7Y3UKJzdk
05	Concyclic feet of focal pedals and product of sums of lengths for odd N	5, 6	OT-xAdbOp8o
06	Invariant altitudes of N-Periodics and outer polygons I	3,4	MvZhWbI6iB8
07	Invariant altitudes of N-Periodics and outer polygon II	5,6	ZMHLmWXeKrM
08	Sum of focal squared altitudes to outer polygon	3–8	VUtBRzmbOYU
09	Sum of square altitudes from arbitrary point to outer polygon	5	RNmHROZNGj8
10	Area products of focal pedal polygons	5	sw8pJFMV00w
11	Area ratios of Pedal Polygons to N-Periodic and outer Polygon	5, 6	6F7Y3UKJzdk
12	Invariant Area Ratios to Minimum-Area Steiner Pedal Polygons	5	f0JwRlu7iaY
13	N-Periodic Inversive Invariants	5	wkstGKq5jOo
14	N-Periodic Inversive Objects	5	bFsehskizls

We achieve this via least-squares optimization [13], available through Mathematica's `FindMinimum[]` function. Namely:

- Initialize N vertices P_i evenly across the ellipse (pick $t_i, i = 1, \ldots, N$ for each), and let $P_1 = (a, 0)$.
- Let b_i be the unit bisector of the N-gon sides incident at P_i. Let n_i denote the ellipse normal at the P_i. The P_i will be a legitimate closed billiard trajectory if all bisectors are perfectly aligned with the local normals, i.e., if P_i^* can be found which make the following error vanish:

$$\mathcal{E} = \sum_{i=1}^{N} (n_i^T . b_i)^2$$

- Obtain the unique confocal ellipse tangent to $[a, 0]P_2^*$.

Notice only $N/2$ vertices for N odd (resp. $N/4$ for N even) need to be optimized if one exploits the symmetries of odd (resp. even) vertex positions when $P_1 = (a, 0)$.

In terms of identifying invariants, we look for quantities which over hundreds of configurations of a given N-family are statistically constant, maintained over a range of Billiard aspect ratios.

5 Video List

Videos of some of the above phenomena have been placed on a Youtube playlist [17] and are listed individually on Table 10.

Acknowledgements We would like to thank Olga Romaskevitch, Sergei Tabachnikov, Richard Schwartz, Arseniy Akopyan, Hellmuth Stachel, Alexey Glutsyuk, Corentin Fierobe, Maxim Arnold, and Pedro Roitman for useful discussions and insights.
The second author is fellow of CNPq and coordinator of Project PRONEX/CNPq/FAPEG 2017 10 26 7000 508.

Appendix

Table 11 Symbols used in the invariants. Note $i = 1, ..., N$ and $j = 1, 2$

Symbol	Meaning
O, N	Center of billiard and trajectory vertices
L, J	Inv. perimeter and Joachimsthal's constant
a, b	Billiard major, minor semi-axes
a'', b''	Caustic major, minor semi-axes
f_1, f_2	Foci
P_i, P_i', P_i''	N-periodic, outer, inner polygon vertices
$d_{j,i}$	Distances from P_i to f_j
l_i, r_i	$\lvert P_i'' - P_i\rvert, \lvert P_{i+1} - P_i''\rvert$
θ_i, θ_i'	N-periodic, outer polygon angles
$\alpha_{j,i}$	Angle $P_i f_j P_{i+1}$
A, A', A''	N-periodic, outer, inner areas
M	A point in the plane of the billiard
Q_i, Q_i'	Feet of perps. from point M to sides of N-periodic, outer polygon
ϕ_i, ϕ_i'	Angle between two consecutive perps. to N-periodic and outer polygon
$Q_i^*, Q_i^{*\prime}$	Vertices of the antipedal polygon from M with respect to the P_i, P_i'
$Q_{j,i}, Q_{j,i}^*$	Vertices of pedal, antipedal polygon wrt. f_j
$q_{j,i}, q_{j,i}^*$	$\lvert Q_{j,i} - f_j\rvert$ and $\lvert Q_{j,i}^* - f_j\rvert$
A_m, A_m', A_m^*	Area of Q_i, Q_i', Q_i^* polygons
A_j, A_j'	Feet of perps. from f_j, $j = 1, 2$ onto the N-periodic, outer polygon
C_0, C_0', C_0^*	Vertex centroids of the Q_i, Q_i', Q_i^* polygons

Table 11 continued

Symbol	Meaning
C_2, C_2', C_2^*	Area centroids of the Q_i, Q_i', Q_i^* polygons
$C_0^{*\prime}, C_2^{*\prime}$	Vertex, area centroids of the $Q_i^{*\prime}$ polygon
K, K', K''	Steiner centroids of curvature of P, P', P''
P_k, P_k', P_k''	Pedal Polygons of P, P', P'' wrt. K, K', K''
A_k, A_k', A_k''	Areas of P_k, P_k', P_k''
$P_{ev}, P_{ev}', P_{ev}''$	Evolute Polygons of P, P', P''
$A_{ev}, A_{ev}', A_{ev}''$	Areas of P_{ev}, P_{ev}', P_{ev}''
$P_{j,i}^{-1}$	Inversion of P_i wrt. to unit-radius circle centered on f_j
$\mathcal{P}_j, L_j$	Polygon whose vertices are $P_{j,i}^{-1}$ and its perimeter
$\gamma_{j,i}$	Internal angle of $\mathcal{P}_j$ at its ith vertex ($P_{j,i}^{-1}$)

References

1. Akopyan, A.: Angles $\phi = \pi - \theta_i$ (resp. $\phi' = \phi - \theta_i'$), so equivalent to invariant sum (resp. product) of cosines. Private Communication (2020)
2. Akopyan, A.: Corollary of Theorem 6 in Akopyan et al., Billiards in Ellipses Revisited (2020). Private Communication (2020)
3. Akopyan, A.: Follows from previous results: the construction is affine and holds for any two concentric conics. Private (2020). Communication
4. Akopyan, A.: Perpendicular feet to N-periodic or its tangential polygon are cyclic. Private (2020). Communication
5. Akopyan, A., Schwartz, R., Tabachnikov, S.: Billiards in ellipses revisited. Eur. J. Math. (2020). https://doi.org/10.1007/s40879-020-00426-9
6. Arnold, M., Fuchs, D., Izmestiev, I., Tabachnikov, S., Tsukerman, E.: Iterating evolutes and involutes. Discrete Comput. Geom. **58**, 80–143 (2017). https://doi.org/10.1007/s00454-017-9890-y
7. Bialy, M., Tabachnikov, S.: Dan Reznik's identities and more. Eur. J. Math. (2020) https://doi.org/10.1007/s40879-020-00428-7
8. Chavez-Caliz, A.: More about areas and centers of Poncelet polygons. Arnold Math J. (2020). https://doi.org/10.1007/s40598-020-00154-8
9. Dragović, V., Radnović, M.: Poncelet Porisms and Beyond: Integrable Billiards, Hyperelliptic Jacobians and Pencils of Quadrics. Frontiers in Mathematics. Basel: Springer (2011)
10. Garcia, R., Reznik, D., Koiller, J.: New properties of triangular orbits in elliptic billiards. Math. Monthly, to appear, Amer (2020)
11. Izmestiev, I., Tabachnikov, S.: Ivory's theorem revisited. J. Integr. Syst. 2. (2017). https://doi.org/10.1093/integr/xyx006
12. Kaloshin, V., Sorrentino, A.: On the integrability of Birkhoff billiards. Phil. Trans. R. Soc. A (376) (2018)
13. Mangasarian, O.L.: Nonlinear Programming. SIAM, New York (1994)
14. Nomizu, K., Sasaki, T.: Affine Differential Geometry. Cambridge University Press, Cambridge (1994)
15. Preparata, F., Shamos, M.: Computational Geometry - An Introduction, 2nd edn. Springer, New York (1988)
16. Reznik, D.: Playlist for Invariants of 3- and 4-Periodics in the Elliptic Billiard. YouTube. (2020). www.bit.ly/3aNqgqU
17. Reznik, D.: Playlist for Invariants of N-Periodics in the Elliptic Billiard. YouTube. (2020). www.bit.ly/2xeVGYw
18. Reznik, D., Garcia, R., Koiller, J.: Can the elliptic billiard still surprise us? Math. Intell. **42**, 6–17 (2020). www.rdcu.be/b2cg1

19. Roitman, P.: Investigation of n-periodic invariants involving the curvature of the ellipse. Private (2020). **Communication**
20. Rozikov, U.A.: An Introduction To Mathematical Billiards. World Scientific Publishing Company, Singapore (2018)
21. Schwartz, R., Tabachnikov, S.: Centers of mass of Poncelet polygons, 200 years after. Math. Intell. **38**(2), 29–34 (2016). https://doi.org/10.1007/s00283-016-9622-9
22. Stachel, H.: Closed form expression for k_{119}. Private (2020). Communication
23. Stachel, H.: Joachmisthal's constant in terms of a, b and a''. Private (2020). Communication
24. Stachel, H.: Proofs for k_{113} and k_{116}. Private (2020). Communication
25. Steiner, J.: Über den Krümmungs-Schwerpunkt ebener Curven. Abhandlungen der Königlichen Akademie der Wissenshaften zu Berlin 19–91 (1838)
26. Tabachnikov, S.: Geometry and Billiards, vol. 30 of Student Mathematical Library. Providence, RI: American Mathematical Society. (2005). www.bit.ly/2RV04CK
27. Weisstein, E.: Mathworld. (2019). www.mathworld.wolfram.com
28. Wolfram, S.: Mathematica, version 10.0 (2019)

Publisher's Note Springer Nature remains neutral with regard to jurisdictional claims in published maps and institutional affiliations.